Inorganic Chemistry

Article

pubs.acs.org/IC

Hybrid Bimetallic Metal–Organic Frameworks: Modulation of the Framework Stability and Ultralarge CO_2 Uptake Capacity

Xiaokai Song, Minhak Oh, and Myoung Soo Lah*

Interdisciplinary School of Green Energy, Ulsan National Institute of Science & Technology, Ulsan, 689-805, Korea

ABSTRACT: A series of isostructural hybrid bimetallic metal–organic frameworks (MOFs), Ni_xM_{1-x}-ITHDs [M = Zn(II), Co(II)], have been prepared via a conventional solvothermal reaction in the presence of varying mole ratios of Ni(II)/Zn(II) or Ni(II)/Co(II) mixed metal ions. While a critical amount of the doped Ni(II) ion (more than ≈0.2 mol fraction) is needed to have any enhancement of the framework stability of the hybrid bimetallic Ni_xZn_{1-x}-ITHDs, even a very small amount of the doped Ni(II) ion (≈0.1 mol fraction) produced a full enhancement of the framework stability of the hybrid bimetallic Ni_xCo_{1-x}-ITHDs. The highly porous and rigid Ni_xCo_{1-x}-ITHDs activated via a conventional vacuum drying process shows a Brunauer–Emmett–Teller specific surface area of 5370 $m^2\ g^{-1}$, which is comparable to that of pure Ni-ITHD. The CO_2 uptake capacities of Ni-ITHD and $Ni_{0.11}Co_{0.89}$-ITHD (2.79 and 2.71 g g^{-1}, respectively) at 1 bar and 195 K are larger than those of any other reported MOFs under similar conditions and the excess CO_2 uptake capacity at 40 bar and 295 K (≈1.50 g g^{-1}) is comparable to those of other MOFs, which are activated via the supercritical carbon dioxide drying process, with similar pore volumes.

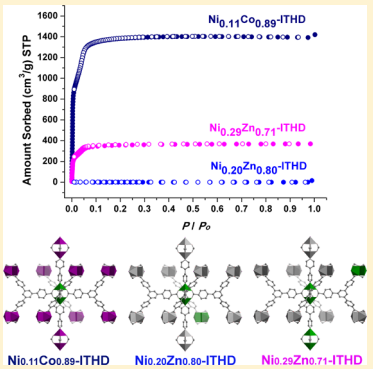

INTRODUCTION

Metal–organic frameworks (MOFs), also known as porous coordination polymers (PCPs), are a class of highly crystalline porous materials that have attracted considerable attention as promising candidates for CO_2 capture because of their unique properties, such as tunable pore dimensions and properties and high specific surface area.[1] Recent interest in CO_2 capture at ambient temperature and pressure has mainly focused on MOFs with open metal sites[2] and functionalized amines.[3] MOFs with extremely large pore volumes and specific surface areas are very important for CO_2 capture at high pressure.[4] Thus, great efforts have been made in the syntheses of new MOFs that could have, in particular, the largest possible pore volumes and specific surface areas. For instance, NU-110/-111[5] and IRMOF-74[6] with nanosized ligands and UMCM-1/-2/-3[7] and Bio-MOF-100[8] with mixed organic linkers have been reported as MOFs with extremely large pore volumes and specific surface areas when they were activated via the supercritical carbon dioxide drying process.[9] However, it is well-known that most MOFs with ultralarge solvent cavities are extremely unstable and show significantly less permanent porosity than the expected porosity from the single-crystal structure or even no permanent porosity when the lattice solvents in the cavity were removed via the conventional vacuum-drying process.[10,11] It is still a great challenge to prepare a stable MOF with ultrahigh porosity.

Heterometallic MOFs have been investigated for the modulation of framework properties, such as the enhancement of framework stability, gas sorption behavior, and catalytic activity and the tuning of breathing behavior, luminescence, and magnetic properties.[12] A general strategy toward heterometallic MOFs, especially bimetallic MOFs, is to use two different metal ions as reactants during the conventional solvothermal reaction process. The reaction of a ligand with two different metal ions sometimes results in a bimetallic MOF as a pure phase rather than a mixture of two homometallic MOFs.[12a,b,d,f,i–k,13]

Recently, a postsynthetic exchange of the metal ion in a known MOF, a transmetalation, offered a new route to bimetallic MOFs.[11,12c,h,l,14] A family of isostructural M-ITHDs {$[M_6(BTB)_4(bipy)_3]$, where M = Zn(II), Co(II), Cu(II), and Ni(II); BTB = benzene-1,3,5-tribenzoate; and bipy = 4,4′-bipyridyl} of a 3,6-connected **ith-d** net topology based on the $M_2(COO)_4$ paddle-wheel secondary building unit (SBU) as a six-connected node and BTB as a three-connected node have been reported.[11] Interestingly, while M-ITHD [where M = Zn(II) or Co(II)] shows no or very low porosity, the isostructural core–shell bimetallic Ni_xM_{1-x}-ITHDs, prepared by selective postsynthetic exchange of the framework metal ions from M(II) to Ni(II), showed partially enhanced porosity or even fully enhanced ultrahigh porosity with a Brunauer–Emmett–Teller (BET) specific surface area comparable to that of pure Ni-ITHD (5590 $m^2\ g^{-1}$), which is, to the best of our knowledge, the largest value among the MOFs activated via the conventional vacuum drying process. Therefore, not only pure Ni-ITHD but also even some core–shell bimetallic Ni_xM_{1-x}-ITHDs could be considered as the most rigid and stable MOFs among the reported MOFs with ultrahigh porosity.

Herein, we report the conventional solvothermal syntheses of a series of hybrid bimetallic Ni_xM_{1-x}-ITHD MOFs of varying metal ratios with enhanced framework stability and ultrahigh porosity via nonselective doping of Ni(II) ion in Zn- and Co-ITHD frameworks and investigate the factors determining the framework stability. We also report the sorption behaviors of

Received: April 5, 2013
Published: September 19, 2013

the hybrid bimetallic Ni_xCo_{1-x}-ITHDs, which have been activated via the conventional vacuum-drying process, including their ultralarge CO_2 uptake capacities at low temperature/ambient pressure and ambient temperature/high pressure.

EXPERIMENTAL SECTION

General Procedures. All reagents used were purchased from commercial sources and used without further purification. Elemental analysis (C, H, and N) was performed at the Central Research Facilities of Ulsan National Institute of Science & Technology. Metal ions (Zn, Co, and Ni) were analyzed using a Varian 720-ES inductively coupled plasma atomic emission spectrometer. FT-IR spectra were recorded using KBr pellets with a Nicolet iS 10 FT-IR spectrophotometer (4000−400 cm^{-1}). Thermal gravimetric analysis (TGA) data were recorded using a TA Instruments Q-600 series thermal gravimetric analyzer under flowing nitrogen gas. Powder X-ray diffraction (PXRD) data were recorded using a Bruker D2 Phaser automated diffractometer at room temperature, with a step size of 0.02° in 2θ angle.

Syntheses of MOFs. A series of Ni-doped isostructural MOFs, Ni_xM_{1-x}-ITHD $\{[Ni_{6x}M_{6(1-x)}(BTB)_4(bipy)_3](DMF)_m(H_2O)_n$, M = Zn(II) and Co(II), where the subscripts x and $1-x$ represent the mole fractions of Ni(II) ion and the other metal ion in the framework, respectively; the subscripts m and n are the numbers of solvent N,N'-dimethylformamide (DMF) and water molecules in the solvent cavity, respectively$\}$, were prepared via solvothermal reactions in the presence of the corresponding mixed metal ions in appropriate mole ratios, which were slightly modified from the reported synthetic procedures.[11]

$Ni_{0.20}Zn_{0.80}$-ITHD. A solid mixture of $Ni(NO_3)_2{\cdot}6H_2O$ (10.1 mg, 0.035 mmol), $Zn(NO_3)_2{\cdot}6H_2O$ (30.9 mg, 0.104 mmol), benzene-1,3,5-tribenzoic acid (H_3BTB) (44.1 mg, 0.101 mmol), and bipy (9.9 mg, 0.063 mmol) was dissolved in 5 mL of DMF. The solution was divided into five portions in Pyrex tubes and heated in an isotherm oven at 100 °C for 3 d, resulting in dark-green rhombic dodecahedral crystals, which were collected by filtration and washed with fresh DMF. Yield: 135 mg, 93.5% based on bipy. Anal. Calcd for $Ni_{1.2}Zn_{4.8}(BTB)_4(bipy)_3(DMF)_{47}(H_2O)_{47}$ = $C_{278}H_{507}O_{118}N_{53}Ni_{1.2}Zn_{4.8}$ (fw = 6876.63 g/mol): C, 48.73; H, 7.43; N, 10.80. Found: C, 48.36; H, 7.18; N, 11.13. FT-IR (KBr, 4000−400 cm^{-1}): 3421 (br, w), 3066 (w), 2929 (w), 1662 (vs), 1609 (s), 1594 (s), 1541 (m), 1388 (vs), 1254 (w), 1220 (w), 1181 (w), 1100 (w), 1070 (m), 1016 (w), 857 (m), 811 (w), 782 (m), 706 (w), 669 (w), 574 (w), 479 (w).

$Ni_{0.29}Zn_{0.71}$-ITHD. The preparation of $Ni_{0.29}Zn_{0.71}$-ITHD was performed by a similar procedure as for $Ni_{0.20}Zn_{0.80}$-ITHD with the mixed metal salts of $Ni(NO_3)_2{\cdot}6H_2O$ (15.1 mg, 0.052 mmol) and $Zn(NO_3)_2{\cdot}6H_2O$ (25.6 mg, 0.086 mmol). Yield: 138 mg, 89.0% based on bipy. Anal. Calcd for $Ni_{1.7}Zn_{4.3}(BTB)_4(bipy)_3(DMF)_{60}(H_2O)_{25}$ = $C_{318}H_{550}O_{107}N_{66}Ni_{1.7}Zn_{4.3}$ (fw = 7391.15 g/mol): C, 51.68; H, 7.50; N, 12.51. Found: C, 51.67; H, 7.26; N, 12.52.

$Ni_{0.38}Zn_{0.62}$-ITHD. The preparation of $Ni_{0.38}Zn_{0.62}$-ITHD was performed by a similar procedure as for $Ni_{0.20}Zn_{0.80}$-ITHD with the mixed metal salts of $Ni(NO_3)_2{\cdot}6H_2O$ (20.1 mg, 0.069 mmol) and $Zn(NO_3)_2{\cdot}6H_2O$ (20.6 mg, 0.069 mmol). Yield: 105 mg, 71.8% based on bipy. Anal. Calcd for $Ni_{2.3}Zn_{3.7}(BTB)_4(bipy)_3(DMF)_{45}(H_2O)_{64}$ = $C_{282}H_{516}O_{120}N_{54}Ni_{2.3}Co_{3.7}$ (fw = 6960.38 g/mol): C, 48.66; H, 7.47; N, 10.87. Found: C, 48.28; H, 7.05; N, 11.12.

$Ni_{0.64}Zn_{0.36}$-ITHD. The preparation of $Ni_{0.64}Zn_{0.36}$-ITHD was performed by a similar procedure as for $Ni_{0.20}Zn_{0.80}$-ITHD with the mixed metal salts of $Ni(NO_3)_2{\cdot}6H_2O$ (30.1 mg, 0.104 mmol) and $Zn(NO_3)_2{\cdot}6H_2O$ (10.5 mg, 0.035 mmol). Yield: 112 mg, 79.4% based on bipy. Anal. Calcd for $Ni_{3.8}Zn_{2.2}(BTB)_4(bipy)_3(DMF)_{45}(H_2O)_{47}$ = $C_{273}H_{493}O_{116}N_{51}Ni_{3.8}Co_{2.2}$ (fw = 6713.05 g/mol): C, 48.85; H, 7.40; N, 10.64. Found: C, 48.55; H, 7.06; N, 10.97.

$Ni_{0.06}Co_{0.94}$-ITHD. The preparation of $Ni_{0.06}Co_{0.94}$-ITHD was performed by a similar procedure as for $Ni_{0.20}Zn_{0.80}$-ITHD with the mixed metal salts of $Ni(NO_3)_2{\cdot}6H_2O$ (2.1 mg, 0.007 mmol) and $Co(NO_3)_2{\cdot}6H_2O$ (38.1 mg, 0.131 mmol). The resulting purple rhombic dodecahedral crystals were collected by filtration and washed with fresh DMF. Yield: 122 mg, 79.5% based on bipy. Anal. Calcd for $Ni_{0.4}Co_{5.6}(BTB)_4(bipy)_3(DMF)_{60}(H_2O)_{20}$ = $C_{318}H_{544}O_{104}N_{66}Ni_{0.4}Co_{5.6}$ (fw = 7309.70 g/mol): C, 52.25; H, 7.50; N, 12.65. Found: C, 51.82; H, 7.23; N, 13.07. FT-IR (KBr, 4000−400 cm^{-1}): 3391 (br, w), 3065 (w), 2932 (w), 1655 (vs), 1607 (s), 1585 (s), 1536 (m), 1389 (vs), 1255 (w), 1220 (w), 1182 (w), 1104 (w), 1069 (m), 1015 (w), 858 (m), 809 (w), 782 (m), 698 (w), 574 (w), 479 (w).

$Ni_{0.11}Co_{0.89}$-ITHD. The preparation of $Ni_{0.11}Co_{0.89}$-ITHD was performed by a similar procedure as for $Ni_{0.20}Zn_{0.80}$-ITHD with the mixed metal salts of $Ni(NO_3)_2{\cdot}6H_2O$ (4.1 mg, 0.014 mmol) and $Co(NO_3)_2{\cdot}6H_2O$ (36.2 mg, 0.124 mmol). Yield: 138 mg, 95.2% based on bipy. Anal. Calcd for $Ni_{0.7}Co_{5.3}(BTB)_4(bipy)_3(DMF)_{43}(H_2O)_{67}$ = $C_{267}H_{519}O_{134}N_{49}Ni_{0.7}Co_{5.3}$ (fw = 6912.45 g/mol): C, 46.39; H, 7.57; N, 9.93. Found: C, 45.98; H, 7.14; N, 10.38.

$Ni_{0.23}Co_{0.77}$-ITHD. The preparation of $Ni_{0.23}Co_{0.77}$-ITHD was performed by a similar procedure as for $Ni_{0.20}Zn_{0.80}$-ITHD with the mixed metal salts of $Ni(NO_3)_2{\cdot}6H_2O$ (10.1 mg, 0.035 mmol) and $Co(NO_3)_2{\cdot}6H_2O$ (30.2 mg, 0.104 mmol). Yield: 108 mg, 73.5% based on bipy. Anal. Calcd for $Ni_{1.4}Co_{4.6}(BTB)_4(bipy)_3(DMF)_{47}(H_2O)_{56}$ = $C_{279}H_{525}O_{127}N_{53}Ni_{1.4}Co_{4.6}$ (fw = 7006.66 g/mol): C, 47.83; H, 7.55; N, 10.59. Found: C, 47.39; H, 7.47; N, 11.00.

$Ni_{0.48}Co_{0.52}$-ITHD. The preparation of $Ni_{0.48}Co_{0.52}$-ITHD was performed by a similar procedure as for $Ni_{0.20}Zn_{0.80}$-ITHD with the mixed metal salts of $Ni(NO_3)_2{\cdot}6H_2O$ (20.1 mg, 0.069 mmol) and $Co(NO_3)_2{\cdot}6H_2O$ (20.2 mg, 0.069 mmol). Yield: 101 mg, 68.7% based on bipy. Anal. Calcd for $Ni_{2.9}Co_{3.1}(BTB)_4(bipy)_3(DMF)_{45}(H_2O)_{64}$ = $C_{273}H_{527}O_{133}N_{51}Ni_{2.9}Co_{3.1}$ (fw = 7005.32 g/mol): C, 46.81; H, 7.58; N, 10.20. Found: C, 46.41; H, 7.30; N, 10.68.

M-ITHD. A series of pure M-ITHDs [M = Zn(II), Co(II), and Ni(II)] was prepared according to the reported procedures.[11]

Gas Adsorption Studies. *Activation of MOFs Using a Conventional Vacuum-Drying Process.* The following specific procedure was used to activate all of the MOFs via the conventional vacuum-drying process. The as-synthesized MOF crystals were soaked in methylene chloride for 2 d; the solvent methylene chloride was refreshed three times during the soaking process. The resulting sample soaked in methylene chloride was transferred as a suspension in a BET sample cell and the solvent was decanted. The wet sample was then evacuated at room temperature under vacuum for 1 d.

Low-Pressure Gas Sorption Measurements. All gas sorption isotherms were measured using a BELSORP-max (BEL Japan, Inc.) employing a standard volumetric technique. The N_2 (with purity of 99.999%) sorption isotherms were monitored at 77 K. The N_2 adsorption data in the pressure range lower than ≈0.15 P/P_0 were fitted to the BET equation to determine the BET specific surface areas. The entire set of the N_2 adsorption data was used to obtain the Langmuir specific surface area. For CO_2 (99.99%) measurements at 195 K, a freezing mixture of dry ice and 2-propanol was used.

High-Pressure CO_2 Sorption Measurements. All high-pressure CO_2 adsorption measurements were performed on a Rubotherm gravimetric sorption analyzer with a magnetic suspension balance at 295 K. Prior to the adsorption measurements, the samples soaked in methylene chloride were transferred to a sample cell and activated for 24 h under vacuum at room temperature. Approximately 0.25 g of sample (after activation) was used for high-pressure CO_2 adsorption measurements.

RESULTS AND DISCUSSION

In this study, we synthesized a series of isostructural hybrid bimetallic MOFs, Ni_xM_{1-x}-ITHDs, via solvothermal reactions of H_3BTB and bipy with varying mole ratios of Ni(II)/Zn(II) or Ni(II)/Co(II) mixed metal ions in DMF at 100 °C. The mole fraction of the doped Ni(II) ion in the bimetallic Ni_xM_{1-x}-ITHD structure can be easily controlled by adjusting the mole ratio of Ni(II)/Zn(II) or Ni(II)/Co(II) in the reactants. As the ratio of the Ni(II) ion increases, the color of the Ni_xZn_{1-x}-ITHD MOF deepens from pale green to dark

dx.doi.org/10.1021/ic400844v | Inorg. Chem. 2013, 52, 10869−10876

green (Figure 1). The optical microscopic photographs of Ni_xZn_{1-x}-ITHD crystals and their face-cut fragments clearly show that the green color from the Ni(II) ion is dispersed throughout the single crystal (Figure 2), which indicates that the doped Ni(II) ions are uniformly incorporated in the framework.

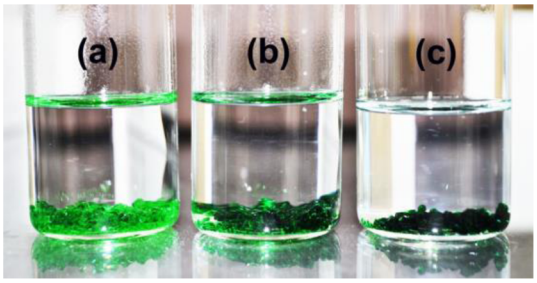

Figure 1. Optical photographs of bulk samples of hybrid bimetallic (a) $Ni_{0.20}Zn_{0.80}$-ITHD, (b) $Ni_{0.38}Zn_{0.62}$-ITHD, and (c) $Ni_{0.64}Zn_{0.36}$-ITHD.

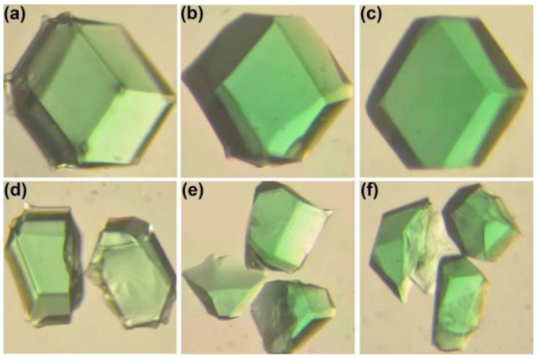

Figure 2. Optical microscopic photographs of a single crystal of hybrid bimetallic (a) $Ni_{0.20}Zn_{0.80}$-ITHD, (b) $Ni_{0.38}Zn_{0.62}$-ITHD, and (c) $Ni_{0.64}Zn_{0.36}$-ITHD, and their corresponding face-cut fragments (d, e, f, respectively).

When the mole ratio of the Ni(II) and Zn(II) ions in the reactants varied from 0.33:1 to 0.60:1, to 1:1, and then to 3:1, the isostructural bimetallic MOFs $Ni_{0.20}Zn_{0.80}$-ITHD, $Ni_{0.29}Zn_{0.71}$-ITHD, $Ni_{0.38}Zn_{0.62}$-ITHD, and $Ni_{0.64}Zn_{0.36}$-ITHD with 0.25:1, 0.41:1, 0.61:1, and 1.78:1 metal ratios, respectively, were obtained (Table 1). The mole fractions of the doped Ni(II) ion in the bimetallic MOFs are smaller than the mole fractions in the corresponding reactants, which suggests that there is a preference for the Zn-based paddle-wheel SBU rather than the Ni-based paddle-wheel SBU. However, when the Ni(II) and Co(II) ions with varying metal mole ratios, 0.05:1, 0.11:1, 0.33:1, and 1:1, were used, the isostructural bimetallic MOFs $Ni_{0.06}Co_{0.94}$-ITHD, $Ni_{0.11}Co_{0.89}$-ITHD, $Ni_{0.23}Co_{0.77}$-ITHD, and $Ni_{0.48}Co_{0.52}$-ITHD with 0.06:1, 0.12:1, 0.30:1, and 0.92:1 metal mole ratios, respectively, were obtained (Table 2). The mole fractions of the doped Ni(II) ion in the bimetallic MOFs are almost the same as the mole fractions in the corresponding reactants, which suggests that there is no preference for either the Ni(II) ion or Co(II) ion in the dinuclear paddle-wheel SBUs.

The bulk identities and the phase purities of the bimetallic MOFs were confirmed by using a combination of elemental analyses and the PXRD patterns of the bimetallic Ni_xM_{1-x}-ITHDs. The PXRD patterns of the Ni-doped bimetallic MOFs are the same as those of pure Zn-ITHD and Co-ITHD (Figure 3).

Ni-ITHD is reported to have better thermal stability than isostructural Zn-ITHD and Co-ITHD.[11] Therefore, the enhanced thermal stabilities of the isostructural bimetallic Ni_xM_{1-x}-ITHDs were expected. However, while the TGA data of the bimetallic Ni_xZn_{1-x}-ITHDs indicate that the thermal behavior of hybrid bimetallic $Ni_{0.20}Zn_{0.80}$-ITHD, $Ni_{0.29}Zn_{0.71}$-ITHD, and $Ni_{0.38}Zn_{0.62}$-ITHD is closer to that of pure Zn-ITHD than that of Ni-ITHD, the thermal behavior of the bimetallic $Ni_{0.64}Zn_{0.36}$-ITHD is closer to that of pure Ni-ITHD than pure Zn-ITHD (Figure 4a). The thermal stability of the Ni_xZn_{1-x}-ITHD is dependent on the mole fraction of the doped Ni(II) ion in the bimetallic structure. Only the Ni_xZn_{1-x}-ITHD with more than 0.60 mol fraction of the doped Ni(II) ion showed significantly improved thermal stability compared with that of pure Zn-ITHD. On the other hand, the TGA data of the bimetallic Ni_xCo_{1-x}-ITHDs are similar to that of pure Co-ITHD (Figure 4b). Even the bimetallic Ni_xCo_{1-x}-ITHD with ≈0.60 mol fraction of the doped Ni(II) ion is not sufficiently thermally stabilized by the Ni(II) ion doping.

The optical microscopic photographs, the PXRD patterns, and the metal ratios in the reactants and in the products of the

Table 1. BET Specific Surface Areas, the Langmuir Surface Areas, and the Total Pore Volumes of Zn-ITHD, Ni-ITHD, Hybrid Bimetallic Ni_xZn_{1-x}-ITHD MOFs and Core−Shell Bimetallic Ni_xZn_{1-x}-ITHD MOFs

ITHD MOFs	Ni/Zn ratio		SA_{BET}[a] ($m^2\ g^{-1}$)	SA_{Lang}[a] ($m^2\ g^{-1}$)	V_p[a] ($cm^3\ g^{-1}$)	ref
	in reactants	in products				
Zn-ITHD	0:1	0:1	0	0	0	11
$Ni_{0.20}Zn_{0.80}$-ITHD_hybrid	0.33:1	0.25:1	0	0	0	this work
$Ni_{0.29}Zn_{0.71}$-ITHD_hybrid	0.60:1	0.41:1	1380	1610	0.57	this work
$Ni_{0.38}Zn_{0.62}$-ITHD_hybrid	1:1	0.61:1	3380	3910	1.42	this work
$Ni_{0.64}Zn_{0.36}$-ITHD_hybrid	3:1	1.78:1	4500	5210	1.85	this work
$Ni_{0.22}Zn_{0.78}$-ITHD_core−shell	–	0.28:1[b]	1230	1320	0.47	11
$Ni_{0.30}Zn_{0.70}$-ITHD_core−shell	–	0.43:1[b]	2320	2420	0.86	11
Ni_1Zn_0-ITHD_core−shell	–	1:0[b]	5310	6020	2.13	11
Ni-ITHD	1:0	1:0	5590	6370	2.25	11

[a]The BET specific surface areas (SA_{BET}) and the Langmuir surface area (SA_{Lang}) of these MOFs activated via the conventional vacuum-drying process obtained from the N_2 adsorption isotherms. The total pore volume (V_p) was estimated from the N_2 adsorption amounts assuming that the density of N_2 in the pores around the saturation pressure at 77 K was the same as that of liquid N_2 at 77 K. [b]The Ni/Zn ratios were modulated via the control of the soaking time in Ni(II) DMF solution during the postsynthetic exchange process.

dx.doi.org/10.1021/ic400844v | Inorg. Chem. 2013, 52, 10869−10876

Table 2. BET Specific Surface Areas, The Langmuir Surface Areas and the Total Pore Volumes of Co-ITHD, Ni-ITHD, Hybrid Bimetallic Ni_xCo_{1-x}-ITHD MOFs, and Core−Shell Bimetallic Ni_xCo_{1-x}-ITHD MOFs

ITHD MOFs	Ni/Co ratio in reactants	Ni/Co ratio in products	SA_{BET}[a] ($m^2\ g^{-1}$)	SA_{Lang}[a] ($m^2\ g^{-1}$)	V_p[a] ($cm^3\ g^{-1}$)	ref
Co-ITHD	0:1	0:1	480	560	0.2	11
$Ni_{0.06}Co_{0.94}$-ITHD_hybrid	0.05:1	0.06:1	4800	5580	2.02	this work
$Ni_{0.11}Co_{0.89}$-ITHD_hybrid	0.11:1	0.12:1	5380	6180	2.17	this work
$Ni_{0.23}Co_{0.77}$-ITHD_hybrid	0.33:1	0.30:1	5360	6200	2.20	this work
$Ni_{0.48}Co_{0.52}$-ITHD_hybrid	1:1	0.92:1	5370	6220	2.21	this work
$Ni_{0.34}Co_{0.66}$-ITHD_core−shell	–	0.52:1[b]	5330	6070	2.15	11
$Ni_{0.49}Co_{0.51}$-ITHD_core−shell	–	0.96:1[b]	5500	6260	2.22	11
Ni_1Co_0-ITHD_core−shell	–	1:0[b]	5330	6110	2.18	11
Ni-ITHD	1:0	1:0	5590	6370	2.25	11

[a]The BET specific surface areas (SA_{BET}) and the Langmuir surface area (SA_{Lang}) of these MOFs activated via the conventional vacuum-drying process obtained from the N_2 adsorption isotherms. The total pore volume (V_p) was estimated from the N_2 adsorption amounts assuming that the density of N_2 in the pores around the saturation pressure at 77 K was the same as that of liquid N_2 at 77 K. [b]The Ni/Co ratios were modulated via the control of the soaking time in Ni(II) DMF solution during the postsynthetic exchange process.

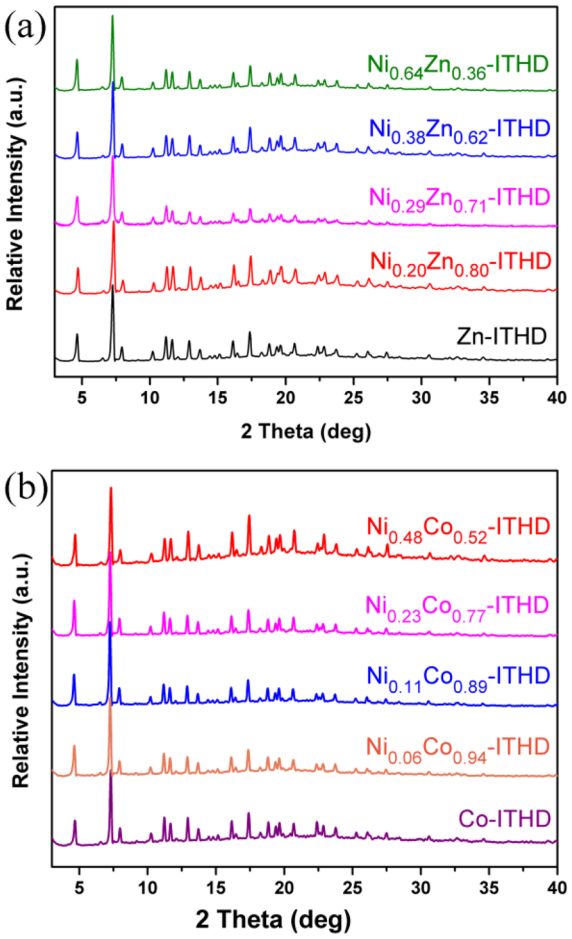

Figure 3. (a) PXRD patterns of as-synthesized Zn-ITHD and the hybrid bimetallic Ni_xZn_{1-x}-ITHDs. (b) PXRD patterns of as-synthesized Co-ITHD and the hybrid bimetallic Ni_xCo_{1-x}-ITHDs.

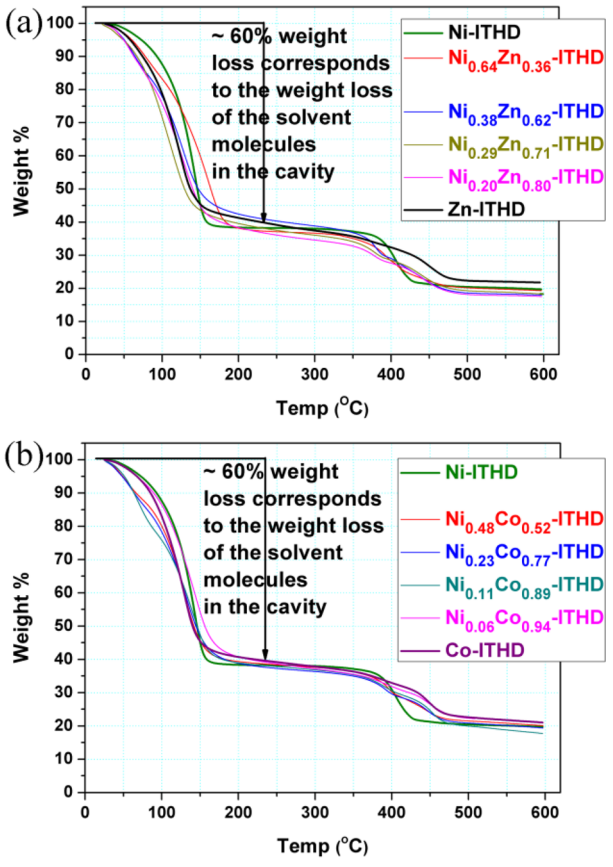

Figure 4. (a) TGA of as-synthesized Zn-ITHD, Ni-ITHD, and the hybrid bimetallic Ni_xZn_{1-x}-ITHDs. (b) TGA of as-synthesized Co-ITHD, Ni-ITHD, and the hybrid bimetallic Ni_xCo_{1-x}-ITHDs.

bimetallic Ni_xM_{1-x}-ITHDs suggest that the MOFs are hybrid structures and will be one of the two different types shown in Figure 5. One could be a hybrid bimetallic Ni_xM_{1-x}-ITHD containing both a heterodinuclear paddle-wheel $NiM(COO)_4$ SBU and a homodinuclear $Ni_2(COO)_4$ and/or $M_2(COO)_4$ SBU without any cooperative Ni(II) ion and/or M(II) ion doping within an SBU (Figure 5a). The other might be the hybrid bimetallic MOF containing only the homodinuclear $Ni_2(COO)_4$ and/or $M_2(COO)_4$ SBU without any heterodinuclear paddle-wheel $NiM(COO)_4$ SBU with cooperative Ni(II) ion and/or M(II) ion doping within an SBU (Figure 5b). The smaller Ni(II)/Zn(II) ratios in the products than in the reactants for Ni_xZn_{1-x}-ITHDs (Table 1) suggest the existence of the cooperative effect for the more homodinuclear $Zn_2(COO)_4$ SBUs in the framework, while the same Ni(II)/Co(II) ratios in the reactants and the products for Ni_xCo_{1-x}-ITHDs (Table 2) suggest the existence of a cooperative effect neither for $Co_2(COO)_4$ nor for $Ni_2(COO)_4$ SBUs.

dx.doi.org/10.1021/ic400844v | Inorg. Chem. 2013, 52, 10869−10876

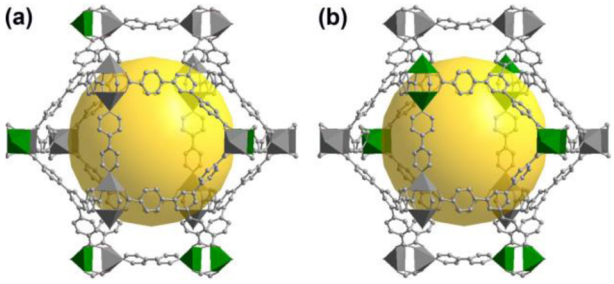

Figure 5. Two proposed hybrid bimetallic Ni_xM_{1-x}-ITHD structures, where M = Zn(II) and Co(II). (a) The framework with both homodinuclear paddle-wheel SBUs $M_2(COO)_4$ and $Ni_2(COO)_4$ and heterodinuclear SBU $NiM(COO)_4$. (b) The framework with only the homodinuclear SBUs. Ni polyhedra (green), Zn, and Co polyhedra (gray).

The higher porosity of the Ni-ITHD framework compared with the Zn-ITHD framework and the enhanced porosity of the core−shell bimetallic Ni_xZn_{1-x}-ITHD frameworks compared with the porosity of the Zn-ITHD framework prompted investigation of the sorption behavior of the hybrid bimetallic Ni_xZn_{1-x}-ITHDs with the expectation of a similar enhanced porosity compared with that of the pure Zn-ITHD framework. Interestingly, while core−shell bimetallic $Ni_{0.22}Zn_{0.78}$-ITHD has enhanced porosity compared with the porosity of pure Zn-ITHD with a N_2 adsorption amount of 302 $cm^3\ g^{-1}$ and a BET specific surface area of 1230 $m^2\ g^{-1}$, hybrid bimetallic $Ni_{0.20}Zn_{0.80}$-ITHD containing a similar amount of the doped Ni(II) ion does not show any N_2 adsorption (Figure 6a,b and Table 1). The ≈0.2 mol fraction of the doped Ni(II) ion in the hybrid bimetallic Ni_xZn_{1-x}-ITHD framework is not enough for any enhancement of the porosity of the framework. In contrast, the N_2 adsorption amount and the BET specific surface area of hybrid bimetallic $Ni_{0.29}Zn_{0.71}$-ITHD are 317 $cm^3\ g^{-1}$ and 1380 $m^2\ g^{-1}$, which are ≈25% of the corresponding values of pure Ni-ITHD; the N_2 adsorption amount and the BET specific surface area of hybrid bimetallic $Ni_{0.38}Zn_{0.62}$-ITHD are 916 $cm^3\ g^{-1}$ and 3380 $m^2\ g^{-1}$, which are ≈60% of the corresponding values of pure Ni-ITHD; and the N_2 adsorption amount and the BET specific surface area of hybrid bimetallic $Ni_{0.64}Zn_{0.36}$-ITHD are 1194 $cm^3\ g^{-1}$ and 4500 $m^2\ g^{-1}$, which are ≈80% of the corresponding values of pure Ni-ITHD. The different behavior in the enhancement of the porosity between the core−shell bimetallic structures and the hybrid bimetallic structures is related to the local mole fractions of the doped Ni(II) ions. The frameworks of the hybrid bimetallic structures are only stabilized when the local mole fraction of the doped Ni(II) ion is larger than a certain threshold value, which is larger than ≈0.20 but smaller than ≈0.29. For core−shell bimetallic $Ni_{0.22}Zn_{0.78}$-ITHD, although the average mole fraction of the doped Ni(II) ion in the framework is only ≈0.2, the local mole fraction of doped Ni(II) ion in the shell region of the crystal is probably larger than the threshold value because of localization of the Ni(II) ion mainly in the shell region, which leads to the enhancement of the porosity to some extent.

In contrast to the lack of any enhancement of the porosity of hybrid bimetallic $Ni_{0.22}Zn_{0.78}$-ITHD, even hybrid bimetallic $Ni_{0.06}Co_{0.94}$-ITHD with only 0.06 mol fraction of doped Ni(II) ion showed a significant enhancement of the framework stability. The BET specific surface area of hybrid bimetallic $Ni_{0.06}Co_{0.94}$-ITHD is 4800 $m^2\ g^{-1}$ (Figure 7a and Table 2),

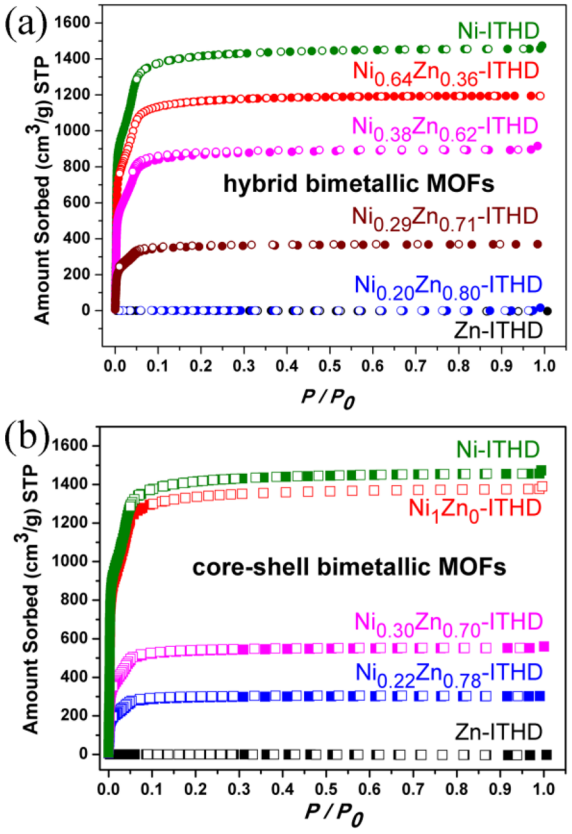

Figure 6. The N_2 sorption isotherms of (a) hybrid bimetallic Ni_xZn_{1-x}-ITHDs (circles) and (b) core−shell bimetallic Ni_xZn_{1-x}-ITHDs[11] (squares) at 77 K. Solid and open shapes represent adsorption and desorption isotherms, respectively.

which corresponds to ≈86% of that of pure Ni-ITHD. Unlike the hybrid bimetallic Ni_xZn_{1-x}-ITHDs, the threshold mole fraction of the doped Ni(II) ion in the hybrid bimetallic Ni_xCo_{1-x}-ITHDs for the enhancement of the porosity is lower than 0.06. All of the BET specific surface areas of the hybrid bimetallic Ni_xCo_{1-x}-ITHD frameworks with Ni(II) mole fractions larger than ≈0.1 are comparable to that of pure Ni-ITHD (Figure 7b and Table 2), which shows that the hybrid bimetallic Ni_xCo_{1-x}-ITHD is much more stable than the corresponding hybrid bimetallic Ni_xZn_{1-x}-ITHD. While the heterogeneous doping of ≈0.2 mol fraction of Ni(II) ion into mainly the shell region of the Zn-ITHD framework leads to some enhancement of the framework stability of core−shell bimetallic Ni_xZn_{1-x}-ITHD,[11] the homogeneous doping of ≈0.2 mol fraction of Ni(II) ion into the Zn-ITHD framework does not lead to any enhancement of the framework stability or to any consequent enhancement of the porosity of the hybrid bimetallic Ni_xZn_{1-x}-ITHD. However, even the homogeneous doping of ≈0.1 mol fraction of Ni(II) ion into the Co-ITHD framework results in significant enhancement of the framework stability and the consequent enhancement of the porosity of hybrid bimetallic Ni_xCo_{1-x}-ITHD, where the enhanced porosity is comparable to the porosity of pure Ni-ITHD.

The stability of a framework is mainly governed by the chemical stability of the metal (or metal cluster as an SBU) node of the framework. The chemical stability of the metal node is strongly influenced by the environments of the metal node, such as the rigidity and the size of the organic nodes connected to the metal node and the number and the type of

dx.doi.org/10.1021/ic400844v | Inorg. Chem. 2013, 52, 10869−10876

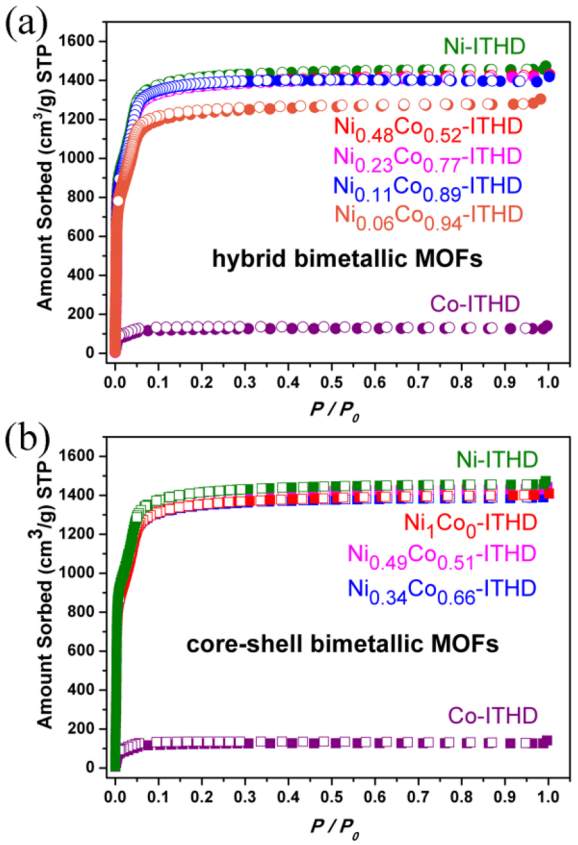

Figure 7. The N_2 sorption isotherms of (a) hybrid bimetallic Ni_xCo_{1-x}-ITHDs (circles) and (b) core–shell bimetallic Ni_xCo_{1-x}-ITHDs[11] (squares) at 77 K. Solid and open shapes represent adsorption and desorption isotherms, respectively.

the surrounding metal nodes interconnected via the organic nodes. The framework stabilities of the pure ITHDs suggest that the order of the inherent stability of the paddle-wheel SBUs is $Ni_2(COO)_4$ > $Co_2(COO)_4$ > $Zn_2(COO)_4$.[11] The N_2 adsorption amount and the BET specific surface area of hybrid bimetallic $Ni_{0.11}Co_{0.89}$-ITHD suggest that not only the $Ni_2(COO)_4$ SBU but also the 10 surrounding $Co_2(COO)_4$ SBUs interlinked via the rigid organic ligands as shown in Figure 8a are stable enough to show a permanent porosity comparable to that of pure Ni-ITHD. The calculated mole fraction of the doped Ni(II) ion in the structure is 0.09, which is in good agreement with the experimental result of ≈0.1 mol

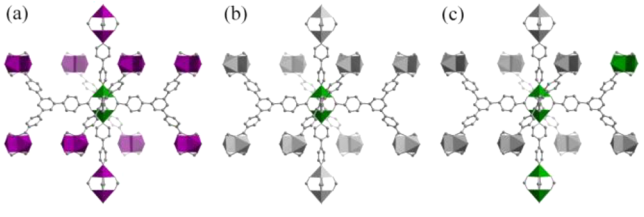

Figure 8. Three local structures around a Ni-based paddle-wheel SBU in hybrid bimetallic Ni_xM_{1-x}-ITHDs, where 10 surrounding paddle-wheel SBUs are interconnected via four BTB and two bipy ligands. (a) All 10 surrounding SBUs are based on a Co-based paddle-wheel SBU. (b) All 10 surrounding SBUs are based on a Zn-based paddle-wheel SBU. (c) More than two among the 10 surrounding SBUs are based on a Ni-based paddle-wheel SBU. Ni polyhedron (green), Co polyhedra (purple), and Zn polyhedra (gray).

fraction of the doped Ni(II) ion in the hybrid bimetallic $Ni_{0.11}Co_{0.89}$-ITHD structure. However, in the hybrid bimetallic Ni_xZn_{1-x}-ITHD MOFs, even the Ni-based paddle-wheel SBU surrounded by all-Zn-based paddle-wheel SBUs (Figure 8b) is not sufficiently stable. To enhance the framework stability, at least some surrounding paddle-wheel SBUs of the Ni-SBU must also be Ni-SBUs (Figure 8c).

The ultrahigh porosity and BET specific surface areas of pure Ni-ITHD and the hybrid bimetallic Ni_xCo_{1-x}-ITHDs make them good candidates for CO_2 capture. The CO_2 sorption isotherms, at 195 K and 1 bar, of pure Ni-ITHD and hybrid bimetallic $Ni_{0.11}Co_{0.89}$-ITHD activated via the conventional vacuum-drying process (Figure 9) are similar to those of other

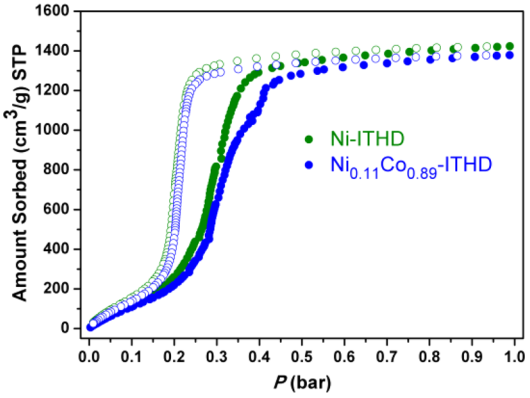

Figure 9. CO_2 sorption isotherms of Ni-ITHD (green) and hybrid bimetallic $Ni_{0.11}Co_{0.89}$-ITHD (blue) at 195 K, where the solid and open shapes represent adsorption and desorption isotherms, respectively.

MOFs with ultralarge porosity.[15−17] The feature of the steep rise in the uptake amounts in the adsorption isotherms around ≈0.3 bar is very close to that of DUT-25,[15] which could be attributed to the condensation of the CO_2 in the mesoporous cavity by attractive electrostatic interaction between the CO_2 molecules. Similar steep rises in the uptake amounts around ≈0.2 bar were also observed in the adsorption isotherms of SNU-77H[16] and Be-BDC with microporous features.[17] The hysteresis in the CO_2 sorption isotherms of pure Ni-ITHD and hybrid bimetallic $Ni_{0.11}Co_{0.89}$-ITHD might be related to the relatively small aperture dimensions of the cagelike mesopores of the M-ITHD structures.[18] The CO_2 uptake amount of hybrid bimetallic $Ni_{0.11}Co_{0.89}$-ITHD is 1379 $cm^3\ g^{-1}$ (2.71 g g^{-1}, 73.0 wt %[19]) at 195 K and 1 bar, which is comparable to that of pure Ni-ITHD, 1423 $cm^3\ g^{-1}$ (2.79 g g^{-1}, 73.6 wt %) (Figure 9 and Table 3). To the best of our knowledge, these CO_2 uptake amounts are much larger than the largest reported values so far, 1105 $cm^3\ g^{-1}$ (2.17 g g^{-1}, 68.5 wt %) for DUT-25, 860 $cm^3\ g^{-1}$ (1.69 g g^{-1}, 62.8 wt %) for SNU-77H, and 815 $cm^3\ g^{-1}$ (1.60 g g^{-1}, 61.5 wt %) for Be-BDC, under similar conditions.

The large CO_2 uptake capacity at ambient temperature/high pressure is also important for CO_2 capture. Both pure Ni-ITHD and hybrid bimetallic $Ni_{0.11}Co_{0.89}$-ITHD have very large CO_2 uptake capacities at ambient temperature. As shown in Figure 10, the isotherms for these MOFs at 295 K are saturated at a pressure of 40 bar. The excess CO_2 uptake amounts of Ni-ITHD and $Ni_{0.11}Co_{0.89}$-ITHD are 1.49 g g^{-1} (759 $cm^3\ g^{-1}$, 59.8 wt %) and 1.45 g g^{-1} (738 $cm^3\ g^{-1}$, 59.2 wt %), respectively (Table 3). These values are smaller than those of MOF-200/-

dx.doi.org/10.1021/ic400844v | Inorg. Chem. 2013, 52, 10869−10876

Table 3. CO_2 Uptakes of Ni-ITHD, Hybrid Bimetallic $Ni_{0.11}Co_{0.89}$-ITHD, and Other MOFs

MOFs	CO_2 uptake ($cm^3\ g^{-1}$, g g^{-1}, wt %) at 195 K (1 bar)	V_p ($cm^3\ g^{-1}$)	excess CO_2 uptake ($cm^3\ g^{-1}$, g g^{-1}, wt %) (pressure, bar)	total CO_2 uptake ($cm^3\ g^{-1}$, g g^{-1}, wt %) (pressure, bar)	temp (K)	ref
MOF-210	nd[a]	3.60	1222, 2.40, 70.6 (50)	1222, 2.48, 71.3 (50)	298	4a
MOF-200	nd	3.59	1222, 2.40, 70.6 (50)	1441, 2.83, 73.9 (50)	298	4a
NU-100	nd	2.82	1040, 2.04, 67.1 (40)	1182, 2.32, 69.9 (40)	298	4b
Ni-ITHD	1423, 2.79, 73.6	2.25	759, 1.49, 59.8 (40)	886, 1.74, 63.5 (50)	295	this work
DUT-25	1105, 2.17, 68.5	2.22	754, 1.48, 59.7 (54)	927, 1.82, 64.5 (54)	298	15
DUT-9	nd	2.18	835, 1.64, 62.1 (47)	nd	298	21
$Ni_{0.11}Co_{0.89}$-ITHD	1379, 2.71, 73.0	2.17	738, 1.45, 59.2 (40)	856, 1.68, 62.7 (50)	295	this work
MOF-205	nd	2.16	764, 1.50, 60.0 (37)	866, 1.67, 62.5 (50)	298	4a
MOF-177	nd	1.89	759, 1.49, 59.8 (42)	nd	298	20
Be-BDC	815, 1.60, 61.5	1.44	nd	nd		17
NOTT-122	nd	1.41	576, 1.13, 53.1(20)	nd	298	22
Cu-TPBTM	nd	1.27	525, 1.03, 50.7 (20)	nd	298	23
SNU-77H	860, 1.69, 62.8	1.17	475, 0.93, 48.2 (40)	nd	298	16
Mg-CPO-27	nd	0.63	331, 0.65, 39.4 (35)	nd	298	24b
Mg-MOF-74	nd	0.57	336, 0.66, 39.8 (40)	336, 0.66, 39.8 (40)	313	24a

[a]No data were reported.

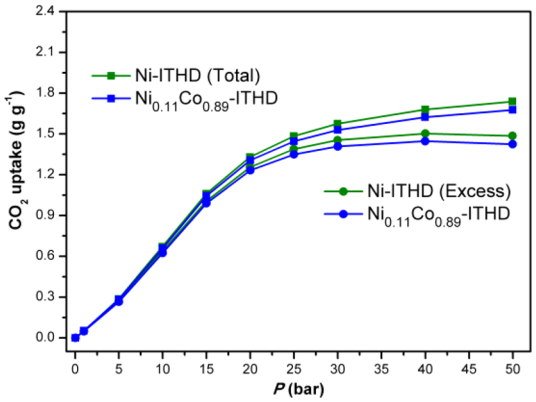

Figure 10. Excess (circle) and total (square) CO_2 uptakes of Ni-ITHD (green) and hybrid bimetallic $Ni_{0.11}Co_{0.89}$-ITHD (blue) at 295 K.

210 (2.40 g g^{-1}, 1222 $cm^3\ g^{-1}$, 70.6 wt %)[4a] and NU-100 (2.04 g g^{-1}, 1040 $cm^3\ g^{-1}$, 67.1 wt %)[4b] with larger pore volumes but are comparable to those of other porous MOFs with similar pore volumes such as MOF-205 (1.50 g g^{-1}, 764 $cm^3\ g^{-1}$, 60.0 wt %),[4a] DUT-25 (1.48 g g^{-1}, 754 $cm^3\ g^{-1}$, 59.7 wt %),[15] MOF-177 (1.47 g g^{-1}, 749 $cm^3\ g^{-1}$, 60 wt %),[20] and DUT-9 (1.64 g g^{-1}, 835 $cm^3\ g^{-1}$, 62.1 wt %)[21] and are larger than those of MOFs famous for high CO_2 uptake capacities at ambient condition with smaller pore volumes, such as Nott-122 (1.13 g g^{-1}, 576 $cm^3\ g^{-1}$, 53.1 wt %),[22] Cu-TPBTM (1.03 g g^{-1}, 525 $cm^3\ g^{-1}$, 50.7 wt %),[23] and Mg-MOF-74 (0.66 g g^{-1}, 336 $cm^3\ g^{-1}$, 39.8 wt %).[24]

CONCLUSIONS

A series of isostructural hybrid bimetallic MOFs, Ni_xM_{1-x}-ITHDs [M = Zn(II), Co(II)], has been prepared via solvothermal syntheses using H_3BTB and bipy ligands with the mixed metal salts. The mole fractions of the doped Ni(II) ion in the hybrid bimetallic Ni_xM_{1-x}-ITHDs could be easily controlled by adjusting the mole ratio of Ni(II)/Zn(II) or Ni(II)/Co(II) under the reaction conditions. The uniform incorporation of the doped Ni(II) ion in the hybrid bimetallic structures as a pure phase without any site selectivity was confirmed from the optical microscopic photographs of the crystals. Even a small mole fraction of the doped Ni(II) ion (≈0.1) in the hybrid bimetallic Ni_xCo_{1-x}-ITHDs could produce a full enhancement of the framework stability with a BET specific surface area comparable to that of pure Ni-ITHD. However, in the case of the hybrid bimetallic Ni_xZn_{1-x}-ITHDs, a critical mole fraction of the doped Ni(II) ion (larger than ≈0.2) is needed to produce any enhancement of the framework stability, and even ≈0.6 mol fraction of doped Ni(II) ion does not lead to a full enhancement of the porosity. The stability of a framework is mainly governed by the chemical stability of the metal SBU, which is strongly influenced by the rigidity and size of the organic nodes connected to the metal SBU, and the number and type of the surrounding metal SBUs interconnected via the organic nodes. In the hybrid bimetallic Ni_xCo_{1-x}-ITHDs, not only the Ni-based but also the Co-based paddle-wheel SBUs interconnected via the organic ligands could be sufficiently stabilized to demonstrate a porosity comparable to that of pure Ni-ITHD. However, in the hybrid bimetallic Ni_xZn_{1-x}-ITHDs, even the Ni-based paddle-wheel SBUs that are not interconnected to any Ni-based paddle-wheel SBUs are not sufficiently stable to show any enhanced framework stability or any enhanced porosity of the framework structures. The CO_2 uptake capacities of pure Ni-ITHD and hybrid bimetallic $Ni_{0.11}Co_{0.89}$-ITHD at 195 K and ambient pressure are the largest among the reported MOFs. The excess CO_2 uptake capacity of both pure Ni-ITHD and hybrid bimetallic $Ni_{0.11}Co_{0.89}$-ITHD at ambient temperature and 40 bar is similar to those of other reported MOFs with similar pore volumes. While most MOFs with ultralarge solvent cavities may have appropriate porosities only when they are activated via the supercritical carbon dioxide drying process, not only pure Ni-ITHD but also hybrid bimetallic $Ni_{0.11}Zn_{0.89}$-ITHD have ultralarge porosity even when they are activated via the conventional vacuum-drying process. The construction of hybrid bimetallic MOFs could be used as a general strategy for the preparation of ultraporous MOFs with enhanced framework stability.

dx.doi.org/10.1021/ic400844v | Inorg. Chem. 2013, 52, 10869−10876

AUTHOR INFORMATION

Corresponding Author

*E-mail: mslah@unist.ac.kr.

Notes

The authors declare no competing financial interest.

ACKNOWLEDGMENTS

This work was supported by NRF-2010-0019408 and NRF-2012R1A2A2A01003077 through the National Research Foundation of Korea.

ABBREVIATIONS

MOFs, metal−organic frameworks; SBU, secondary building unit; BET, Brunauer−Emmett−Teller; TGA, thermal gravimetric analysis; PXRD, powder X-ray diffraction; BTB, 1,3,5-benzenetribenzoate; bipy, 4,4′-bipyridyl; DMF, *N*,*N*′-dimethylformamide.

REFERENCES

(1) Sumida, K.; Rogow, D. L.; Mason, J. A.; McDonald, T. M.; Bloch, E. D.; Herm, Z. R.; Bae, T.-H.; Long, J. R. *Chem. Rev.* **2012**, *112*, 724.

(2) (a) Britt, D.; Furukawa, H.; Wang, B.; Glover, T. G.; Yaghi, O. M. *Proc. Natl. Acad. Sci. U. S. A.* **2009**, *106*, 20637. (b) Yazaydın, A. Ö.; Snurr, R. Q.; Park, T.-H.; Koh, K.; Liu, J.; LeVan, M. D.; Benin, A. I.; Jakubczak, P.; Lanuza, M.; Galloway, D. B.; Low, J. J.; Willis, R. R. *J. Am. Chem. Soc.* **2009**, *131*, 18198. (c) Lee, Y.-G.; Moon, H. R.; Cheon, Y. E.; Suh, M. P. *Angew. Chem., Int. Ed.* **2008**, *47*, 7741.

(3) (a) McDonald, T. M.; Lee, W. R.; Mason, J. A.; Wiers, B. M.; Hong, C. S.; Long, J. R. *J. Am. Chem. Soc.* **2012**, *134*, 7056. (b) Demessence, A.; D'Alessandro, D. M.; Foo, M. L.; Long, J. R. *J. Am. Chem. Soc.* **2009**, *131*, 8784.

(4) (a) Furukawa, H.; Ko, N.; Go, Y. B.; Aratani, N.; Choi, S. B.; Choi, E.; Yazaydın, A. Ö.; Snurr, R. Q.; O'Keeffe, M.; Kim, J.; Yaghi, O. M. *Science* **2010**, *329*, 424. (b) Farha, O. K.; Yazaydin, A. O.; Eryazici, I.; Malliakas, C. D.; Hauser, B. G.; Kanatzidis, M. G.; Nguyen, S. T.; Snurr, R. Q.; Hupp, J. T. *Nat. Chem.* **2010**, *2*, 944.

(5) (a) Farha, O. K.; Eryazici, I.; Jeong, N. C.; Hauser, B. G.; Wilmer, C. E.; Sarjeant, A. A.; Snurr, R. Q.; Nguyen, S. T.; Yazaydın, A. Ö.; Hupp, J. T. *J. Am. Chem. Soc.* **2012**, *134*, 15016. (b) Farha, O. K.; Wilmer, C. E.; Eryazici, I.; Hauser, B. G.; Parilla, P. A.; O'Neill, K.; Sarjeant, A. A.; Nguyen, S. T.; Snurr, R. Q.; Hupp, J. T. *J. Am. Chem. Soc.* **2012**, *134*, 9860.

(6) Deng, H.; Grunder, S.; Cordova, K. E.; Valente, C.; Furukawa, H.; Hmadeh, M.; Gandara, F.; Whalley, A. C.; Liu, Z.; Asahina, S.; Kazumori, H.; O'Keeffe, M.; Terasaki, O.; Stoddart, J. F.; Yaghi, O. M. *Science* **2012**, *336*, 1018.

(7) (a) Koh, K.; Wong-Foy, A. G.; Matzger, A. J. *Angew. Chem., Int. Ed.* **2008**, *47*, 677. (b) Koh, K.; Wong-Foy, A. G.; Matzger, A. J. *J. Am. Chem. Soc.* **2009**, *131*, 4184. (c) Koh, K.; Wong-Foy, A. G.; Matzger, A. J. *J. Am. Chem. Soc.* **2010**, *132*, 15005.

(8) An, J.; Farha, O. K.; Hupp, J. T.; Pohl, E.; Yeh, J. I.; Rosi, N. L. *Nat. Commun.* **2012**, *3*, 604.

(9) (a) Nelson, A. P.; Farha, O. K.; Mulfort, K. L.; Hupp, J. T. *J. Am. Chem. Soc.* **2009**, *131*, 458. (b) Farha, O. K.; Hupp, J. T. *Acc. Chem. Res.* **2010**, *43*, 1166.

(10) (a) Ma, L.; Falkowski, J. M.; Abney, C.; Lin, W. *Nat. Chem.* **2010**, *2*, 838. (b) Song, X.; Zou, Y.; Liu, X.; Oh, M.; Lah, M. S. *New J. Chem.* **2010**, *34*, 2396. (c) Deshpande, R. K.; Minnaar, J. L.; Telfer, S. G. *Angew. Chem., Int. Ed.* **2010**, *49*, 4598. (d) Wang, H.-N.; Meng, X.; Yang, G.-S.; Wang, X.-L.; Shao, K.-Z.; Su, Z.-M.; Wang, C.-G. *Chem. Commun.* **2011**, *47*, 7128.

(11) Song, X.; Kim, T. K.; Kim, H.; Kim, D.; Jeong, S.; Moon, H. R.; Lah, M. S. *Chem. Mater.* **2012**, *24*, 3065.

(12) (a) Burrows, A. D. *CrystEngComm* **2011**, *13*, 3623. (b) Li, H.; Shi, W.; Zhao, K.; Li, H.; Bing, Y.; Cheng, P. *Inorg. Chem.* **2012**, *51*, 9200. (c) Dincă, M.; Long, J. R. *J. Am. Chem. Soc.* **2007**, *129*, 11172. (d) Botas, J. A.; Calleja, G.; Sanchez-Sanchez, M.; Orcajo, M. G. *Langmuir* **2010**, *26*, 5300. (e) Yang, H.; He, X.-W.; Wang, F.; Kang, Y.; Zhang, J. *J. Mater. Chem.* **2012**, *22*, 21849. (f) Nouar, F.; Devic, T.; Chevreau, H.; Guillou, N.; Gibson, E.; Clet, G.; Daturi, M.; Vimont, A.; Greneche, J. M.; Breeze, M. I.; Walton, R. I.; Llewellyn, P. L.; Serre, C. *Chem. Commun.* **2012**, *48*, 10237. (g) Cahill, C. L.; de Lill, D. T.; Frisch, M. *CrystEngComm* **2007**, *9*, 15. (h) Huang, S.; Li, X.; Shi, X.; Hou, H.; Fan, Y. *J. Mater. Chem.* **2010**, *20*, 5695. (i) Bo, Q. B.; Wang, H. Y.; Wang, D. Q.; Zhang, Z. W.; Miao, J. L.; Sun, G. X. *Inorg. Chem.* **2011**, *50*, 10163. (j) Yan, C.; Li, K.; Wei, S. C.; Wang, H. P.; Fu, L.; Pan, M.; Su, C. Y. *J. Mater. Chem.* **2012**, *22*, 9846. (k) Yang, H.; Li, T.-h.; Wang, F.; Zhang, J. *Inorg. Chem. Commun.* **2012**, *16*, 86. (l) Kim, Y.; Das, S.; Bhattacharya, S.; Hong, S.; Kim, M. G.; Yoon, M.; Natarajan, S.; Kim, K. *Chem.—Eur. J.* **2012**, *18*, 16642.

(13) (a) Wang, Y.; Cheng, P.; Chen, J.; Liao, D.-Z.; Yan, S.-P. *Inorg. Chem.* **2007**, *46*, 4530. (b) Lim, C.-S.; Schnobrich, J. K.; Wong-Foy, A. G.; Matzger, A. J. *Inorg. Chem.* **2010**, *49*, 5271. (c) Zheng, S.-T.; Wu, T.; Zuo, F.; Chou, C.; Feng, P.; Bu, X. *J. Am. Chem. Soc.* **2012**, *134*, 1934. (d) Zheng, S.-T.; Wu, T.; Chou, C.; Fuhr, A.; Feng, P.; Bu, X. *J. Am. Chem. Soc.* **2012**, *134*, 4517. (e) Caskey, S. R.; Matzger, A. J. *Inorg. Chem.* **2008**, *47*, 7942. (f) Brozek, C. K.; Dincă, M. *Chem. Sci.* **2012**, *3*, 2110.

(14) (a) Das, S.; Kim, H.; Kim, K. *J. Am. Chem. Soc.* **2009**, *131*, 3814. (b) Prasad, T. K.; Hong, D. H.; Suh, M. P. *Chem.—Eur. J.* **2010**, *16*, 14043. (c) Yao, Q.; Sun, J.; Li, K.; Su, J.; Peskova, M. V.; Zou, X. *Dalton Trans.* **2012**, *41*, 3953. (d) Song, X.; Jeong, S.; Kim, D.; Lah, M. S. *CrystEngComm* **2012**, *14*, 5753. (e) Mi, L.; Hou, H.; Song, Z.; Han, H.; Xu, H.; Fan, Y.; Ng, S. W. *Cryst. Growth Des.* **2007**, *7*, 2553. (f) Mukherjee, G.; Biradha, K. *Chem. Commun.* **2012**, *48*, 4293. (g) Mi, L.; Hou, H.; Song, Z.; Han, H.; Fan, Y. *Chem.—Eur. J.* **2008**, *14*, 1814. (h) Shultz, A. M.; Sarjeant, A. A.; Farha, O. K.; Hupp, J. T.; Nguyen, S. T. *J. Am. Chem. Soc.* **2011**, *133*, 13252. (i) Zhang, Z.; Zhang, L.; Wojtas, L.; Nugent, P.; Eddaoudi, M.; Zaworotko, M. J. *J. Am. Chem. Soc.* **2012**, *134*, 924.

(15) Grünker, R.; Bon, V.; Heerwig, A.; Klein, N.; Müller, P.; Stoeck, U.; Baburin, I. A.; Mueller, U.; Senkovska, I.; Kaskel, S. *Chem.—Eur. J.* **2012**, *18*, 13299.

(16) Park, H. J.; Lim, D. W.; Yang, W. S.; Oh, T. R.; Suh, M. P. *Chem.—Eur. J.* **2011**, *17*, 7251.

(17) Porter, W. W.; Wong-Foy, A.; Dailly, A.; Matzger, A. J. *J. Mater. Chem.* **2009**, *19*, 6489.

(18) Thommes, M.; Smarsly, B.; Groenewolt, M.; Ravikovitch, P. I.; Neimark, A. V. *Langmuir* **2006**, *22*, 756.

(19) The gas adsorption capacity of MOF is often expressed in wt % (especially for H_2 and CO_2). While most researchers report the gas adsorption capacity using the wt % definition of (weight of adsorbed gas)/(weight of sample + weight of adsorbed gas), some others report it in the other inappropriate wt % definition, (weight of adsorbed gas)/(weight of sample). Because of confusion on the wt % definition, it is safe to express the gas adsorption capacity in other units such as cm^3/g, mg/g (or g/g), and mmol/g. Here, we used to the wt % unit of (weight of adsorbed gas)/(weight of sample + weight of adsorbed gas) together with the g/g unit and cm^3/g unit for the gas adsorption capacity. See the suggestion on the unit of the gas adsorption capacity in a recent review: Suh, M. P.; Park, H. J.; Prasad, T. K.; Lim, D.-W. *Chem. Rev.* **2012**, *112*, 782.

(20) Millward, A. R.; Yaghi, O. M. *J. Am. Chem. Soc.* **2005**, *127*, 17998.

(21) Gedrich, K.; Senkovska, I.; Klein, N.; Stoeck, U.; Henschel, A.; Lohe, M. R.; Baburin, I. A.; Mueller, U.; Kaskel, S. *Angew. Chem., Int. Ed.* **2010**, *49*, 8489.

(22) Yan, Y.; Suyetin, M.; Bichoutskaia, E.; Blake, A. J.; Allan, D. R.; Barnett, S. A.; Schröder, M. *Chem. Sci.* **2013**, *4*, 1731.

(23) Li, B.; Zhang, Z.; Li, Y.; Yao, K.; Zhu, Y.; Deng, Z.; Yang, F.; Zhou, X.; Li, G.; Wu, H.; Nijem, N.; Chabal, Y. J.; Lai, Z.; Han, Y.; Shi, Z.; Feng, S.; Li, J. *Angew. Chem., Int. Ed.* **2012**, *51*, 1412.

(24) (a) Herm, Z. R.; Swisher, J. A.; Smit, B.; Krishna, R.; Long, J. R. *J. Am. Chem. Soc.* **2011**, *133*, 5664. (b) Dietzel, P. D. C.; Besikiotis, V.; Blom, R. *J. Mater. Chem.* **2009**, *19*, 7362.